Construction and Building Materials 163 (2018) 471–481

Contents lists available at ScienceDirect

Construction and Building Materials

journal homepage: www.elsevier.com/locate/conbuildmat

Durability studies on fiber-reinforced EAF slag concrete for pavements

Vanesa Ortega-López [a,*], José A. Fuente-Alonso [b], Amaia Santamaría [c], José T. San-José [c], Ángel Aragón [a]

[a] Department of Civil Engineering, University of Burgos, EPS, Calle Villadiego s/n, 09001 Burgos, Spain
[b] Department of Construction, University of Burgos, EPS, Calle Villadiego s/n, 09001 Burgos, Spain
[c] Department of Metallurgical Engineering and Materials Science, University of the Basque Country, ETSIB, Alameda Urquijo s/n, 48013 Bilbao, Spain

HIGHLIGHTS

- Steel reinforcement fibers imply lower porosity, permeability and drying shrinkage.
- Fiber-reinforced EAFS concrete performed well in freeze-thaw and wet-dry tests.
- Fiber-reinforced EAFS concrete resisted sulfates and industrial environments.
- EAFS concrete slabs performed well after weathering for five-years outdoors.

GRAPHICAL ABSTRACT

ARTICLE INFO

Article history:
Received 27 July 2017
Received in revised form 6 November 2017
Accepted 15 December 2017

Keywords:
EAF slag concrete
Fiber-reinforced concrete
Durability
Aggressive atmospheres
Weathering
Mercury intrusion porosimetry

ABSTRACT

The long-term behavior of fiber-reinforced hydraulic concretes for pavement applications is studied in this paper. These concretes are manufactured with Electric Arc Furnace Slag as aggregate and exposed to aggressive environments. Mechanical properties, porosity, capillary structure, and long-term variations in length are measured in compressive, tensile, Mercury Intrusion Porosimetry, Fagerlund, and shrinkage tests. The concrete samples are subjected to conventional durability – freeze/thaw and moist-dry – tests and exposed to aggressive agents as sulfates, carbon dioxide, and sulfidic atmospheres with good results. Finally, a set of concrete slabs prepared outdoors are successfully left to weather under detrimental conditions.

1. Introduction

The vast amount of natural aggregates consumed in both construction and civil engineering prompts us to search for alternative materials that can replace natural resources. Furthermore, the use of recycled aggregates in construction and building applications contributes to savings on waste disposal. This philosophy of a circular economy and industrial symbiosis is in line with European Union policies that promote sustainability and environmental assessment in the construction sector [1,2]. A wide range of recycled aggregates has recently been introduced in replacement of natural aggregate for various construction applications [3,4], among which hydraulic [5–8] and bituminous mixtures [9–13], highlighting the use of several types of slags from metallurgical processes in industrial production [14–18].

* Corresponding author.
E-mail address: vortega@ubu.es (V. Ortega-López).

https://doi.org/10.1016/j.conbuildmat.2017.12.121

Over recent decades, the steelmaking industry in Europe has been transformed, in such a way that Electric Arc Furnace (EAF) steelmaking technology has partially replaced outdated blast furnace – LD converters. EAF technology is used for around 30% of European carbon and low alloy steel production. In Spain alone, approximately 70% of all steel is produced in electric arc furnaces (10 MT per year of EAF steel), representing around 15% of total European EAF steel (67 MT per year) [19,20]. The practical use of electric furnaces in steelmaking is divided into two stages: the primary melting-oxidizing processes and the secondary-reducing processes. In the first, an Electric Arc Furnace will generate slag (EAFS) in proportions of 150–180 kg per ton of steel and, in the second, a Ladle Furnace will produce slag (LFS) in proportions of 60–80 kg per ton of steel.

In relation to the above, several studies were carried out to characterize both EAFS [21–25] and LFS [26–34], in addition to the manufacture of hydraulic mixes with EAF slag: mortar [35], plain concrete [36–42], structural and reinforced concrete [43–50] and self-compacting concrete [51,52].

The use of artificial (metallic or synthetic) fibers in the reinforcement of concrete [53–62] poured in situ, carrying the weight of indoor-outdoor wheeled-rolled traffic, has been presented as a good solution for industrial pavements in factories and storehouses. Among other advantages such as stiffness, long-term dimensional stability, cleanliness, liquid absorption, abrasion resistance, toughness and surface fatigue resistance, the easy use of fibers in construction and easy substitution-recycling have greatly enhanced their popularity; several research groups around the world have contributed to advancements in this field. Hence, the use of fibers in this application is a solid engineering solution in substitution of reinforcing steel bars (rebars) in elements submitted to moderate tensile stress, as happens with these ballast-supported paving elements [63,64].

Some of the authors of this paper have recently published a previous study [65], which may be considered directly related to the present paper, on fiber-reinforced concrete made with electric arc furnace slag (CEAFS) used in industrial pavement slabs. They studied its mixtures and performance, prioritizing the engineering aspects of the problem, to go on to conclude that CEAFS reinforced with about 0.5% by volume of metallic or synthetic fibers achieved good mechanical behavior, in terms of strength, toughness and post-cracking behavior; as well as satisfactory abrasion resistance for its use in pavements and concrete ground slabs withstanding rolling traffic. However, issues in that work relating to both the physical and the chemical durability of these concretes were not resolved and these questions now form the subject of the present study, in which the presence of fibers and steelmaking slags and their effects are analyzed.

Studies in the literature (including those of the present authors) generally define the durability of CEAFS (without fibers) as acceptable, though slightly lower than the durability of conventional concrete, especially in terms of carbonation and sulfate attack [40,66] and in freezing/thawing tests [67,68]; results that are attributed to the high porosity of EAFS and, in consequence, the higher permeability of the CEAFS. Researchers in Italy [69] evaluated the durability of concretes manufactured with EAFS in terms of freezing/thawing, wetting/drying, and accelerated aging in hot water. They concluded that it was similar to conventional concretes; however, resistance to chloride-ion permeation of the EAFS concrete was enhanced, observing improvements in the durability of the concretes exposed to chloride environments and lower diffusion coefficients. Probably the main variable inducing differences between the results of the various research teams in the world is the quality of the slag.

The experience of the present team in this field has contributed to satisfactory results in the aforementioned tests and in others (sulfate attack, aggregate-alkali reaction); results that are attributed to good adhesion between the slag aggregate and the surrounding concrete matrix; however, the results obtained for the CEAFS in cases of exposure to marine environments, seawater and chloride penetration tests were not as good as those of the conventional concrete.

In this study, CEAFS with and without fiber reinforcement were manufactured for comparative purposes, to understand the way in which CEAFS containing slag and fibers behave over time, even in the presence of aggressive industrial indoor-outdoor environments. Several in-fresh and in-hardened state properties of CEAFS such as consistency, density, compression, flexion and splitting tension strengths and their elastic moduli are included in this study (showing slightly different values than those detailed in the aforementioned article [65] of the authors), to contribute an overall understanding of the context. Mercury Intrusion Porosimetry (MIP), permeability and porosity tests were performed together with long-term shrinkage evaluation of the mixes. The aggressive environmental conditions under consideration in this work due to their relevance were as follows: freezing/thawing cycles, wetting/drying cycles, sulfate-containing water attack, and exposure to atmospheres rich in gaseous carbon dioxide and sulfur dioxide. Evaluation tests of compressive strength, dimensions, weight, and variations in the external appearance of the mixes performed under those environmental conditions are reported with explanations of the behavior that was observed.

Finally, a number of full-scale slabs were manufactured with these types of concrete and exposed to regional weather conditions (rain, freezing, insolation…) in a five-year weathering process, after which their characteristics and final state were also evaluated.

2. Materials

- *Cement, water, admixtures and natural aggregates*: Ordinary Portland cement (OPC) CEM I/42.5R (EN 197-1:2001 [70]) with a density of 3.1 Mg/m^3, and mix water from the urban mains supply of the city of Burgos (Spain) were employed. The plasticizer admixture was a modified poly-carboxylate polymer and the natural rounded siliceous aggregate was provided as a fine fraction 0/4 mm, fineness modulus (f.m.) 2.5, water absorption 1.4% and oven dry density 2.65 Mg/m^3, the main component of which was SiO_2 (96%).
- *Fibers*: Metallic steel fibers of 50 mm in length, with a density of 7.9 Mg/m^3, a length/diameter aspect ratio of 45, and synthetic fibers of 50 mm in length composed of polyolefin (polypropylene), with a density of 0.92 Mg/m^3, and a length/diameter aspect ratio of 50 were used. The tensile strengths and the moduli of the steel fibers and the synthetic fibers were, respectively, 1000 MPa with a modulus of 210 GPa and 400 MPa with a modulus of 5 GPa.
- *Electric Arc Furnace Slag (EAFS)*: The crushed and weathered EAFS used in this research was supplied by a slag recycling plant in three size fractions (EN 933-1 [70]), 0/4 mm (f.m. 3.3), 4/10 mm (f.m. 5.5), and 10/20 mm (f.m. 7.1). A summary of the main properties are shown here, as the information on grading curves, and both the physical and the chemical properties of the EAFS, together with the characteristics of the natural aggregates, have previously been described in detail in a previous paper [62]. The EAFS used in this work had a density value of about 3.5 Mg/m^3, a water absorption rate of 3.5%, Los Angeles wear loss of under 24% and a flakiness index of under 3%. Almost 75% by weight of the slag aggregate was formed of Fe, Ca and Si oxides, in addition to 20% of Al, Mg, Mn oxides and 5% of other oxides (K_2O, Na_2O, P_2O_5, and TiO_2). Compounds associated with expansive processes, such as free lime and free

magnesia, were below 0.5% and 0.1%, respectively, with no significant volumetric instabilities associated with lime and periclase hydration.

3. Experimental procedure

3.1. Mix-design

The dosage used in the present study, based on the Fuller ideal grading curve, was similar to the dosage described in the previous article in which the optimal fiber amounts were estimated at 0.5% of metallic and synthetic fibers by volume fraction of concrete. These concretes contained aggregate mass proportions of approximately 78% of EAFS and 22% of siliceous sand; the rounded form of these grains of sand partially counteracted the surface roughness effect of the EAFS, slightly improving concrete workability and flowability.

In view of the poor workability of the fiber-reinforced CEAFS described in the previous article, a slight increase in the water/cement ratio of the mixes to 0.55 was introduced before the durability test, to compensate the higher water absorption of the dry EAFS (in our case about 60 additional liters per cubic meter of concrete), thereby obtaining good workability for casting both the laboratory samples and the full-scale outdoor slabs.

Under the above-mentioned conditions, three slag concrete mixes were prepared, in order to evaluate how the fibers affected the durability of the CEAFS. The reference mixture, without fibers, was labeled E, the mixture with metallic fibers, EM, and the mixture with synthetic fibers, ES. Table 1 shows the compositions of the mixtures under study and their consistency, fresh density and the results of the Abrams cone slump test.

The results of the Abrams cone slump test were higher than those in the previous work of the authors, reflecting the fluid consistencies of the CEAFS without fibers and with metallic fibers. On the other hand, CEAFS reinforced with synthetic fibers had a soft almost plastic consistency, as the efficiency of the plasticizer admixture was lower in this case and required slight vibration when preparing slabs. However, the soft-plastic consistency is not a serious drawback for the construction of the pavement slabs that are proposed in this study; if pumping should be required for concrete pouring, a slight increase in water at 5% is a viable alternative.

Due to the greater specific gravity of the EAFS with regard to the natural aggregate, the fresh densities of the CEAFS mixes were higher than those of the conventional concretes. The introduction of fibers slightly increased the density to around 1%.

3.2. Specimen preparation and testing program

The mixing sequence involved a blend of aggregates, followed by the addition of cement, water, plasticizer, and fibers. Subsequently, the different types of specimens were prepared and cured in a climate chamber at temperature of 20 ± 2 °C and relative humidity of 95 ± 5% over different periods depending on the tests. Batches of 60 L were used to prepare the laboratory tests. The three real slabs poured outdoors had dimensions of 2.5 × 2.5 × 0.15 m batched in 900 L per mixture.

The mechanical properties of the hardened concretes (E, EM, ES) were measured in compressive and splitting tensile strength tests using 150 × 300 mm cylindrical specimens. Long-term shrinkage of the 70 × 70 × 280 mm samples was also assessed. Most of the durability tests were performed on 100 mm cubic specimens.

The numerical results of the tests represented an average of, at least, three samples that showed consistent values. The standard deviation is also shown in brackets alongside these values. Finally, Mercury Intrusion Porosimetry (MIP) and Fagerlund surface capillarity tests were also performed.

4. Physical characterization

4.1. Mechanical properties of hardened concrete

Table 2 includes the average strengths and elastic moduli of the three concrete mixes.

The compressive strength test was performed at 7 days, 28 days and 90 days of age; CEAFS mixes in general showed good compressive strengths, with values higher than 55 MPa after 28 days; strength development over time demonstrated a long-term strength gain in all mixes [38,40].

At all curing ages, the compressive strength of mix EM with metallic fibers was always higher than that of mix E with no fibers. However, the compressive strength of mix ES with synthetic fibers at 28 days was similar to that of the reference mix, E, subsequently showing a poorer evolution at 90 days. This behavior could be explained by the chemical admixture that interacts with the fiber polyolefins and affects cement hydration as a "medium-term retardant". Hence, the authors consider that the ES mixture has the "potential to improve" its mechanical strength over time; a theory that will be confirmed following durability tests in the presence of moisture that can act as a curing factor.

Splitting tensile strength was evaluated at 60 days of age. As expected, mix EM (6.94 MPa) and mix ES (5.42 MPa) both improved their spitting tensile strengths with respect to the reference mix, E (4.20 MPa), increasing by more than 65% and 29%, respectively. Despite the lower than expected compressive strength in the ES mix, its obvious gain in tensile strength in comparison with mix E largely compensated that disadvantage with regard to its engineering application in pavement construction (ballast-supported and submitted to slight tensile stress).

The elastic modulus of E and ES mixtures were relatively close, but the value of EM was larger than the former, following the trend in compressive strength; mix ES showed the lowest compressive

Table 1
Mix proportions of concrete and workability.

Mix design (kg/m^3)		E	EM	ES
Cement		360	360	360
Water		200	200	200
Siliceous aggregates (0/4 mm)		500	500	500
EAFS aggregates	Size 0/4 mm	515	515	515
	Size 4/10 mm	670	670	670
	Size 10/20 mm	550	550	550
Plasticizer (1.5% wt. of cement)		5.4	5.4	5.4
Metallic/Synthetic Fibers		–	45	3.5
Abrams cone slump (mm)		140	130	60
Consistency		Fluid	Fluid	Soft
Fresh density (Mg/m^3)		2.86	2.87	2.85

Table 2
Strength and elastic modulus of the concrete mixes (standard deviation in brackets).

Property		Concrete Mix		
		E	EM	ES
Compressive Strength (MPa)	7 days	46.1 (1.6)	60.3 (1.2)	53.3 (1.5)
	28 days	58.8 (2.3)	68.9 (2.1)	57.7 (1.9)
	90 days	72.1 (2.2)	80.6 (1.8)	62.5 (2.0)
Elastic modulus (GPa)	60 days	36 (1.2)	40 (1.5)	34 (1.4)
Splitting Tensile Strength (MPa)	60 days	4.20 (0.9)	6.94 (0.8)	5.42 (1.1)
Dry density (Mg/m^3)	–	2.46	2.53	2.45

strength and the lowest elastic modulus. In general, the values were coherent with those reported in previous works.

4.2. MIP analysis

The concrete matrix porosity, a determining factor in both the mechanical properties and the durability of cement-based materials, was measured by Mercury Intrusion Porosimetry (MIP) on moist-cured samples for 90-days. An Autopore IV 9500 apparatus (Micromeritics) at a pressure of 33,000 psi was used to analyze the volume of pores and the evolution of pore distribution. The results of the MIP analysis, shown in Table 3, revealed porosity values for CEAFS within the range of 10–13%; standard values in well-performed concrete mixes.

The lower porosity in the fiber mixes, EM (10.3%) and ES (11.5%), with respect to the mix without fibers E (12.3%), represents a concrete matrix slightly more compacted in the reinforced concrete after the compaction of fresh samples. Furthermore, the lower porosity of mix EM explains its higher compressive strength (80.6 MPa) and lower variation of weight and strength after the durability tests. The results of the test also suggested the good durability of mix ES.

Fig. 1a represents the pore size frequency of the mixes in terms of differential intrusion; Fig. 1b shows somewhat similar results for all the mixes for cumulative intrusion and global porosity in the fraction sized over than 0.2 microns. Mix ES shows a peak size at 4 microns of medium importance, probably due to the effect of synthetic fibers. A significant peak in the vicinity of 100 nm was shown in the concrete without fibers, more prominent than in the other mixes that negatively influence its durability against physical and chemical agents.

4.3. Water absorption by surface capillarity

Water absorption by surface capillarity, as a measure of both mix permeability to water and pore interconnectivity, was measured on cylindrical (diameter 150 mm, height 70 mm) specimens, cured over 28 days, as per the Fagerlund method described in standard UNE 83982 [71]. The samples were "conditioned" before this test in terms of their initial moisture content, as specified in standard UNE 83966 [71]; thereafter their initial moisture content was about 60–65% of their total water absorption capacity.

Table 3
Results of MIP test and water absorption by capillarity of concrete mixes.

Property	Concrete Mix		
	E	EM	ES
MIP porosity (%)	12.3	10.3	11.5
Water absorption by surface capillarity (g)	66.4	48.7	61
K Capillary absorption coefficient (g/(m^2 * min$^{1/2}$))	0.31	0.195	0.24
ε_e Effective porosity of concrete (cm^3/cm^3)	0.054	0.0395	0.0493
m Resistance to water penetration by capillary absorption (min/cm^2)	308	411	414

The Fagerlund method takes into consideration three values; first, the resistance to water penetration, m; second, the effective porosity, ε; and third, the capillary absorption coefficient, K. The first value is representative of the resistance (inverse of speed) to water permeation, expressed as time divided by the square of penetration height; the second represents the available porosity of concrete that can be filled by water; and, the third is a global characteristic of the capillary process, where the lower the K coefficient, the lower the global capillary absorption.

In Fig. 2, the mass of water gained by the mixes in these tests is shown against the square root of time, which is the usual evaluation of time in Darcy's law. It appears evident that water penetration in mix E (initial slope) is the quickest. The results of effective porosity shown in Table 3 are reasonably lower than the porosity reading of the MIP analysis, due to the initial moisture of samples prescribed in the Fagerlund test; the proportion between both was around 0.4 units (5.4/12.3; 3.95/10.3; 4.93/11.5); water absorption by surface capillarity during that test (in grams) is specified in the second row of the data in Table 3.

In Table 3, the lowest capillary absorption coefficient K (the best result, denoting the lowest level of pore interconnectivity and low permeability) can be seen to correspond to the mix with metallic fibers, EM, and the worst corresponds to the reference mix E, the most permeable mix against water; this information helps foresee the results of the durability tests described in the following sections. The higher permeability of mix E against water is coherent with the distribution of pores given by MIP, in this case 0.1 µm, the most favorable pore size for water diffusion.

4.4. Long-term shrinkage

The long-term shrinkage of the CEAFS mixtures was evaluated on prismatic specimens the dimensions of which were 70 × 70 × 280 mm. These samples are slightly smaller than the recommended size, to test dimensional variations of concrete with maximum aggregate sizes of 20 mm, but our interest centers on validating the influence of fibers on shrinkage. In view of the durability of pavements and slabs made with this type of concrete, a long-term shrinkage ratio smaller than 0.5 thousandth (millimeter per meter) is a positive factor that prevents the appearance of cracks outside the shrinkage joints. It appears reasonable to consider that any eventual presence of cracks or crevices due to shrinkage will always be a negative factor that facilitates access by external aggressive environments (mainly transported by water) and physical and chemical attack.

The length variation of the samples was periodically measured in a rigid frame equipped with a length measuring apparatus. Fig. 3 shows the shrinkage evolution over a period of three months; each point is the average shrinkage ratio of three samples of each mix.

In general, the presence of fibers led to slightly lower shrinkage than mixtures without reinforcement. The presence of fibers embedded in the mass of concrete produced reductions in the long-term value from 0.52 mm/m in mix E to 0.49 mm/m in mix ES and 0.42 mm/m in mix EM. In view of its durability, mix E

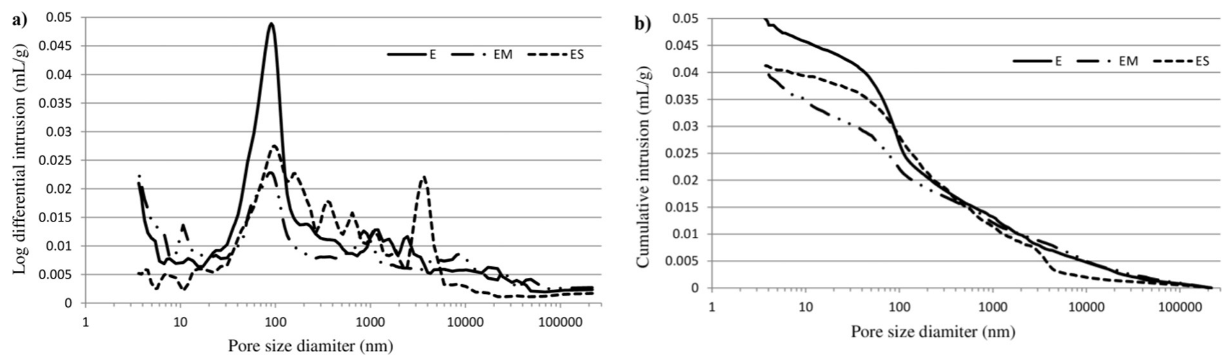

Fig. 1. a) MIP pore size frequency in terms of differential intrusion; b) MIP cumulative intrusion in mixes.

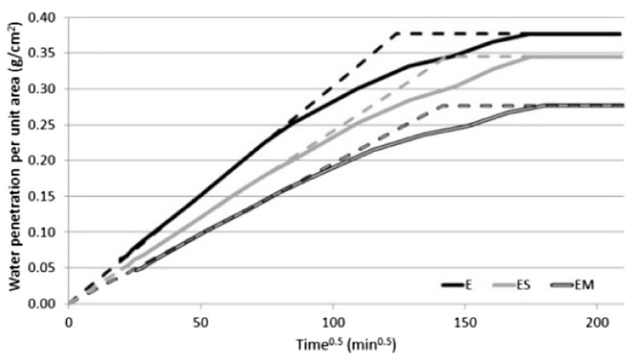

Fig. 2. Water absorption in mixes by capillary action.

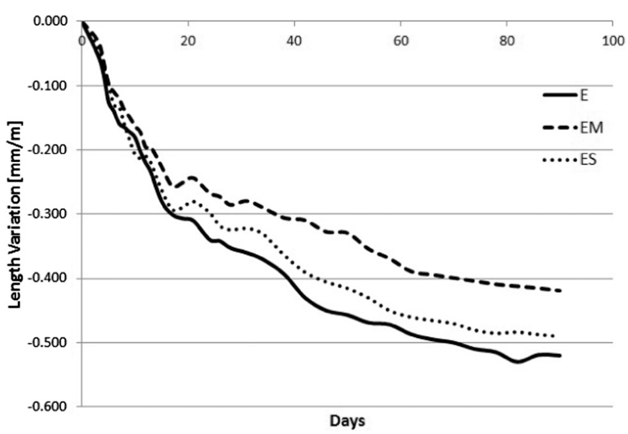

Fig. 3. Shrinkage contraction of concrete specimens.

(without fibers) should be more sensitive to external attack than mixes ES and EM.

5. Durability of hardened concrete

Concrete durability is dependent on its own properties and the potential aggressive agents of the surrounding environment. The durability of the concrete specimens, from a practical and an engineering viewpoint, was evaluated by the following tests.

5.1. Freezing and thawing test

As specified in EN 12390-9 EX [70], three 100 mm cubic specimens of each mix were cured for 90 days in a moist chamber and placed in stainless steel containers filled with an aqueous solution of 3% sodium chloride, simulating a real winter outdoor environment; the samples were subjected to 56 cycles of freezing and thawing. A full cycle of 24 h consisted of 16 h in a freezer at -29 ± 1.2 °C, followed by 8 h of immersion in recirculating solution at 20 ± 1 °C. Periodical measurements of sample mass and temperatures were taken throughout the test, after which the surface appearance and the final variation in weight were reported. The compressive strength and the ultrasound propagation speed were evaluated after the test. The mean results obtained in each of these measures are listed in Table 4.

Before starting the cycles, the samples were "conditioned" so that their initial moisture content was in accordance with standard UNE 83966 [71]. Subsequently, the solution absorption of each mix following immersion for 24 h was measured. The results in Table 4 show that mix E without fibers had the highest absorption (0.70%), followed by the mix with synthetic fibers ES (0.51%), while the mix with metallic fibers has the lowest absorption (0.39%); these results were coherent with those obtained in the Fagerlund test.

A temperature sensor was placed in the center of one sample of each mix type. Fig. 4 represents the evolution of the temperature for mix E sample throughout a typical cycle and the limits established in the standard EN 12390-9 [70]. It can be seen that the temperature between 6 and 14 h showed only minimum differences with regard to the requirements of the standards, due to the lower thermal conductivity of the slag concrete with respect to the conventional concrete; this circumstance allows us to consider the obtained results as admissible.

The internal pressure of ice in the accessible pores of the mixes accompanied by the thermal changes and the sodium chloride presence produced apparent spalling in the specimens. After 28 cycles, the loss of material was evident from the rounded edges of reference mix E. As can be seen in Table 4, mix E suffered a drastic mass loss (−62.41%) implying total destruction after 56 cycles; in fact, after about 35 cycles the appearance of the three samples was qualified as "total cracking", and the posterior mass detachments throughout the cycles are considered as random results. Mixes ES (−4.49%) and EM (−2.92%) showed a lower loss of mass, maintaining their cubic shape. These results are decisive in the durability evaluation of the concrete pavements.

The compressive strength test after 56 cycles was only performed on the EM and the ES concrete specimens, due to the failure of all the E specimens during the test. As may be seen in Table 4, the slight damage to the EM concrete samples led to a decrease in their compressive strength of 3.4%, while the ES concrete samples showed a higher compressive strength (+0.9%) than before the freeze/thaw cycles. This circumstance is probably due to two simultaneous effects: a favorable delayed cement hydration added to damage due to the severity of the test.

As a quality index, the ultrasound pulse velocity was evaluated on dry specimens before and after the freeze/thaw cycles, as

Table 4
Properties of slag concretes after freezing and thawing cycles.

Freezing and thawing test	No. Cycles	Mix		
		E	EM	ES
Absorption after the first 24 h (%)	–	0.70 (0.20)	0.39 (0.10)	0.51 (0.07)
Weight Variation (%)	0–7 cycles	−0.72 (0.30)	−0.06 (0.04)	−0.10 (0.10)
	7–14 cycles	−5.31 (1.6)	−0.30 (0.15)	−0.72 (0.20)
	14–28 cycles	−2.98 (1.02)	−0.72 (0.22)	−1.05 (0.32)
	28–42 cycles	−32.18 (3.10)	−0.77 (0.50)	−1.36 (0.67)
	42–56 cycles	−21.22 (2.10)	−1.07 (0.35)	−1.26 (0.21)
	Total after 56 cycles	−62.41 (3.21)	−2.92 (0.15)	−4.49 (0.75)
Surface appearance	7 cycles	Spalling of the surface	Slight spalling of the surface	
	14 cycles	Loss of surface material	Severe spalling of the surface	
	28 cycles	Rounded edges	Loss of apparent fines	
	42 cycles	Loss of cube form	Loss of surface material	
	56 cycles	Severe damage: samples destroyed, integrity lost	Clear damage: Loss of apparent material	
Ultrasonic Speed (km/s)	0 cycles	4.61 (0.75)	4.78 (0.80)	4.67 (0.77)
	56 cycles	–	4.65 (0.46)	4.68 (0.68)
Compressive Strength (MPa)	0 cycles	72.1 (2.2)	80.6 (1.8)	62.5 (2.0)
	56 cycles	–	77.8 (2.31)	63.1 (1.6)
Variation of Compressive Strength after 56 cycles (%)		−100	−3.4	+0.9

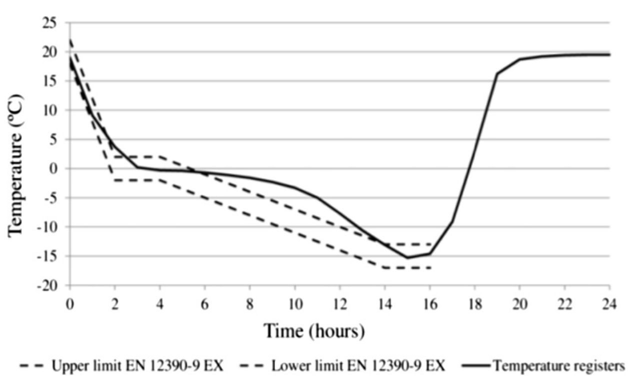

Fig. 4. Temperature records for mix E.

specified in EN 12504-4 [70], (see Fig. 5). The results in Table 4 show that this velocity was coherent with the variations in compressive strength; a slight decrease was clear in mix EM, while the velocity was almost constant in mix ES. An acceptable explanation of this behavior is increased micro-cracking of the concrete matrix. The dynamic stiffness values of the mixes (calculated by the formula $E = 0.9\, v^2/\rho$) notably exceeded the static Young's modulus values shown in Table 2; this circumstance is coherent with the behavior of conventional materials that show increased stiffness at high vibration frequencies.

5.2. Wetting-drying test

This test was guided by the ASTM D-559 standard [72], although standard procedure was not rigorously followed. Three 100 mm cubic specimens from each mix were cured for 90 days in a moist chamber and then subjected to 30 wetting-drying cycles simulating high levels of rainfall. A full cycle of 24 h involved sample immersion in fresh (not saline) water at room temperature for 16 h, followed by forced drying in an oven at 60 °C for 8 h. After the test, the surface appearance of the samples was verified; the final weight variation was reported and compressive tests on all samples were performed. The treatment might be considered detrimental to the mechanical properties of the concretes, because of the combined effect of expansion and contraction, due to thermal variations and to variations in inner and surface humidity levels. Table 5 shows the results obtained after the wetting-drying test.

All the concrete mixes showed good surface appearance and slight weight gains, probably corresponding to slight hydration of some components; additional detrimental micro-cracking of the matrix is likely due to the severity of the test. The oxidation of surface fibers can be seen in mix EM. The loss of compressive strength is appreciable in the mix without fibers. E (−15.2%); however, the mix with metallic fibers showed a lower strength loss (−1.1%). The mix with synthetic fibers clearly increased its strength (+12.1%). It therefore appears logical to assume that the ES mix reached a reasonable strength level during this test (and probably during the freezing-thawing test), enhanced by progressive hydration of the

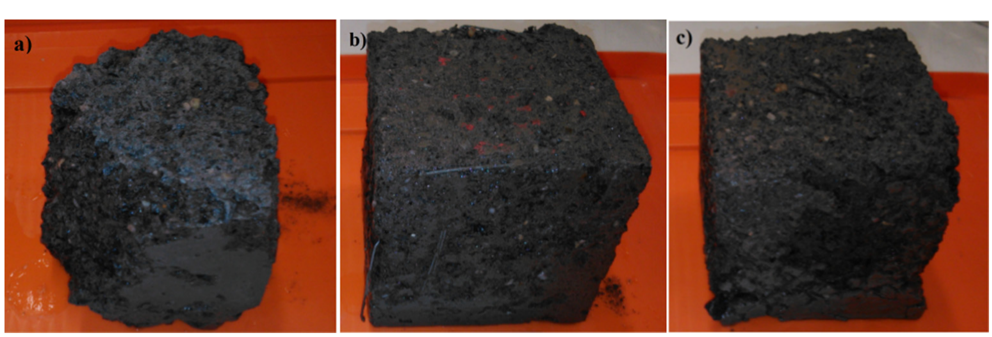

Fig. 5. Superficial appearance of the specimens after 56 freezing/thawing cycles: a) mix E; b) mix EM; c) mix ES.

Table 5
Properties of slag concretes after wetting-drying cycles.

Wetting and Drying test	No. Cycles	Mix		
		E	EM	ES
Weight Variation (%)	30 cycles	+0.23 (0.02)	+0.14 (0.15)	+0.34 (0.10)
Surface appearance	30 cycles	Good	Good	Good
Compressive Strength (MPa)	0 cycles	72.1 (2.2)	80.6 (1.8)	62.5 (2.0)
	30 cycles	61.15 (2.15)	79.65(2.60)	70.12 (3.65)
Variation of Compression Strength after 30 cycles (%)		−15.2	−1.1	+12.1

binder, although slightly reduced by the detrimental effects of the aggressive tests.

Considering the results in both this section and the preceding one, the durable behavior of the fiber-reinforced concrete against natural weathering under outdoor conditions may be described as excellent. These satisfactory results reflected the good internal cohesiveness that existed between the aggregates and the fibers within these slag concrete matrices.

5.3. Sulfate attack test

It is well known that the reaction between sulfate ions and other cement and slag components (Al_2O_3, CaO) can be detrimental to concrete. Taking into account that the concrete mixes under study were proposed for use in pavements and slabs, the sulfate attack test was important, due to the high likelihood of contact between the concrete material and gypsum-containing soils or sulfate-rich subterranean water. Additionally, salt expansion during drying causes internal stresses that could contribute to the deterioration of the concrete structure.

Following the ASTM C 1012 standard [72], three cubic specimens of 100 mm of each concrete sample cured for 90 days in a moist chamber were subjected to 15 cycles of immersion in a water solution of 14% Na_2SO_4–$10H_2O$. A full cycle of 24 h consisted of 5 h immersion in this solution, followed by 17 h of drying in an oven at 110 °C and 2 h of cooling. After the cycles, variations in both the weight and the edge lengths were reported. Their surface appearance and the compressive strength were also verified and the results are shown in Table 6.

The weight increase was lower in mix EM (+0.65%) than in mixes ES (+0.75%) and E (+1.68%). The variation in the length of the cubes, following the expansive effects of the sodium sulfate crystallization and the eventual formation of expansive salts, was the same for mixes E and EM (+0.09%); both results were under the threshold (0.10%) established in the ASTM C 1012 [72] standard for sulfate resistant concretes. However, mix ES (+0.11%) slightly exceeded this threshold. The surface appearance of all the samples was good, with less surface roughness than the samples before the test. Oxide stains on the EM samples were observed.

The compressive strength decreased in mixes E (−16%) and EM (−8.8%), as was expected; once again, the mix with no fibers was more susceptible to deterioration than the mix containing reinforcement fibers; the presence of fibers in the concrete mass being a favorable factor for the durability of concrete.

The compressive strength of mix ES (+9.6%) increased, as in the former freezing-thawing and wetting-drying tests. Once again, the arguments for delayed hydration of binder, not completely reached during its 90-days curing in a moist room, could be repeated here.

5.4. Resistance to gaseous environments (CO_2 and SO_2)

Two tests were proposed to estimate concrete durability in aggressive gaseous environments. First, the test in a chamber of concentrated CO_2 atmosphere, as per the specifications of EN 13295 [70], to determine concrete resistance to carbonation.

Cubic specimens of 100 mm, cured for 90 days in a moist room, were placed in a climatic chamber to simulate accelerated aging. The specimens were left for 56 days in an atmosphere with CO_2 concentrations of 5–20%, at a constant relative humidity of 50–60% and a temperature of 20 ± 2 °C. Every week, the chamber was open and its atmosphere was renewed with CO_2 in maximum concentrations of 20%; it was verified that this concentration decreased by more than 5% over the following days. Once the test period was over, the weight variation and the depth of carbonation were evaluated. To do so, after breaking the specimens into two pieces, carbonation was determined with the method specified in UNE 112011 [71], by applying phenolphthalein over the broken surfaces. Phenolphthalein turns reddish-purple at pH values of over 9.5, indicating that there has been no carbonation in the concrete; and it remains colorless for pH values of less than 8, signaling carbonation. The color is usually light pink at values of between 8 and 9.5. Table 7 shows the values of maximum, average and minimum carbonation depth, the average carbonated area, and the weight variations of the specimens. Fig. 6 shows the carbonated area (colorless) and the non-carbonated area (purple color) of the concretes after the application of phenolphthalein on all the concrete mixes; a thin blue line delimits both areas.

The results showed that all the mixes underwent a similar decrease in weight, probably due to the loss of initial humidity acquired in the moist chamber at 95% RH. The observations revealed that the presence of fibers gave the slag concrete a slightly greater resistance to carbonation than the concrete without fibers. CO_2 penetration into the concrete depends on its permeability; this phenomenon is highly related to the porosity of the mixes and the presence of capillary water in which CO_2 is easily dissolved. Fortunately, mix EM has the best protection against corrosion.

Secondly, we performed the Kesternich test, described in the EN ISO 6988 standard [70], which simulates an industrial atmosphere containing SO_2. The samples used in the test were cubes of 100 mm cured for 90 days in a moist room. The samples were exposed to fifteen 24-h cycles; each cycle included exposure to water vapor saturated in SO_2 at 40 ± 2 °C for 8 h in the chamber, followed by air-cooling at room temperature for 16 h. The detrimental effect of this test on the cementitious matrix consists in the expansive formation of ettringite and thaumasite [73]. Other additional effects could be the oxidation of the metallic particles incrusted in the slag and the oxidation of the metallic fibers in mix EM.

A visual inspection of the samples and measurement of their weight variations and compressive strength were conducted to evaluate the damage and the results are shown in Table 7. After this durability test, the appearance of the samples was good, with small stains and rust points on the surface caused by corrosion. The same chemical activity also caused the slightly increased weight of the samples, with the following variations: +1.36% for mix E; +1.45% for mix EM; and +1.38% for mix ES. With regard to compressive strength, mixes E (−7.7%) and EM (−8.5%) underwent similar loss of strength, revealing harmful effects in the internal structure of the mixes associated with the aforementioned expansive chemical reactions of this test. Mix ES (+6.4%) increased its compressive strength after the test for the same reasons mentioned in the

Table 6
Properties of slag concretes after sulfate attack test.

Sulfate attack test	No. Cycles	Mix		
		E	EM	ES
Weight Variation (%)	15 cycles	+1.68 (0.10)	+0.65 (0.09)	+0.75 (0.12)
Dimensional Variation (%)	15 cycles	+0.09 (0.01)	+0.09 (0.01)	+0.11 (0.01)
Surface appearance	15 cycles	Good	Oxidized fibers	Good
Compressive Strength (MPa)	0 cycles	72.1 (2.2)	80.6 (1.8)	62.5 (2.0)
	15 cycles	60.54 (1.90)	73.47 (2.10)	68.51 (2.30)
Variation of Compressive Strength after 15 cycles (%)		−16	−8.8	+9.6

Table 7
Properties of slag concretes after the resistance to CO_2 atmosphere test and the Kesternich test.

			Mix		
			E	EM	ES
Resistance to CO_2 atmosphere (56 days)	Weight Variation (%)		−2.62 (0.30)	−2.50 (0.25)	−2.78 (0.41)
	Depth of carbonation (mm)	Minimum	5.3 (1.20)	1.1 (1.00)	2.9 (1.00)
		Average	6.2 (1.30)	4.4 (1.25)	5.1 (1.20)
		Maximum	9.0 (1.30)	7.4 (1.50)	13.1 (1.10)
	Carbonated area (%)		22.8 (1.20)	8.1 (1.30)	20.2 (1.50)
Resistance to Kesternich test (15 cycles)	Weight Variation (%)		+1.36 (0.30)	+1.45 (0.90)	+1.38 (0.50)
	Variation of Compression Strength (%)		−7.7	−8.5	+6.4

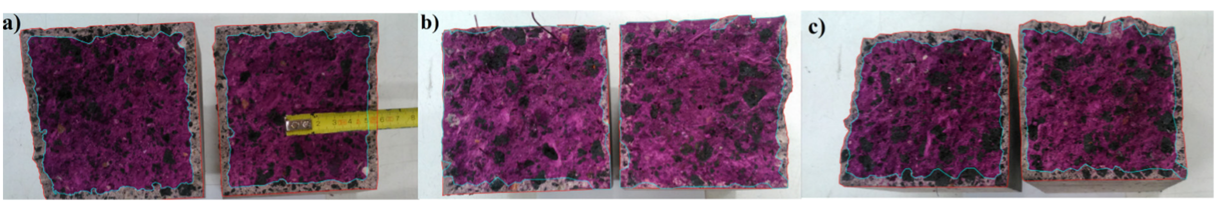

Fig. 6. Definition of carbonated area following the application of phenolphthalein: a) mix E; b) mix EM; c) mix ES. (For interpretation of the references to colour in this figure legend, the reader is referred to the web version of this article.)

preceding sections (enhancement due to delayed curing and simultaneously the harmful effects of the aggressive Kesternich test).

6. Outdoor exposure

Three slabs, one per mix design described in the previous sections, were manufactured using a different type of plasticizer than the one used in the laboratory mixes. The intention of the authors was to avoid undesired interactions between polymeric fibers and the former admixture that produced the delayed retardance of compressive strength gains observed in mixture ES between 28 and 90 days. Slabs were prepared outside the laboratory, under "real" manufacturing conditions (0.9 cubic meters per batch, industrial mixer of 1.2 m^3, batch weight of around 2.5 tons of fresh concrete, slab dimensions of 2.5 × 2.5 × 0.15 m), instead of the 60-L laboratory mixes, at the engineering faculty, Burgos, Spain.

The slab made with mix E was reinforced with two steel grids (Φ6 mm bars) positioned in a classic way to build pavement slabs; the remainder of the slabs had only fiber reinforcements. Fresh concrete was poured on the frameworks and was vibrated for a short time to eliminate entrapped air. A polyethylene sheet was placed between the preexisting pavement and slabs to prevent any adherence of the slab to the floor. After finishing the casting process, the upper surface of the slabs was coated with a "finishing" layer (6 kg of mortar per square meter, with thicknesses varying between 1 and 5 mm, and the upper surface polished by mechanical scrubbing) to facilitate the cleaning and the rolling of trolleys or other vehicles; this layer is usually performed with a mortar the main properties of which are smoothness, hardness, stiffness and resistance to abrasion. The mortar used in this finishing layer is a fluid mixture in which the proportion of binder to aggregate is 1:2 in mass, with a type-I PC cement and a 0–0.6 mm crushed-milled quartz-corundum aggregate. In all, three industrial pavement slabs of more than 6 square meters were built under real conditions for exposure to weathering.

The slabs were weathered outdoors for five years (casting October 2011 – testing November 2016) before evaluating the deterioration of each concrete mixture. In Table 8, the climatology and high temperature fluctuations of the city of Burgos is shown. In winter, sub-zero temperatures are common at night; in summer, the air temperature reach values close to 30 °C during the day. The temperature variation between day and night is usually more than 15 degrees. In this climatology, the slabs were exposed to snow, ice, fog, rain and severe sunshine; the weathering test is used to evaluate the durability of the concrete against adverse climatic conditions. After five years of exposure, the slabs were visually checked and several cores were cut and extracted to evaluate the compressive strength and the impact strength of the three concrete mixes.

6.1. Visual inspection

It is worth mentioning that no slab showed excessive cracking. In the slabs manufactured with concrete mixes E and EM, apparent crazing was observed, see Fig. 7a, and the presence of such flaws was higher in the slab manufactured with mix E (about 20% of the upper surface) than in mix EM (less than 5% of surface). This crazing affected only the finishing layer (at a depth of less than

Table 8
Climatology of the city of Burgos-Spain (AEMET. http://www.aemet.es/).

Month	T	TM	Tm	R	H	DR	DS	DF	DH	I
January	3.1	7.0	−0.8	44	85	7.5	4.7	6.8	18.0	86
February	4.1	9.0	−0.8	35	77	6.9	3.7	3.8	17.2	116
March	7.0	12.9	1.1	34	69	6.1	2.8	1.6	12.3	175
April	8.6	14.4	2.7	61	69	9.2	1.9	1.1	6.6	185
May	12.2	18.4	5.9	63	67	9.3	0.3	1.5	1.1	226
June	16.5	23.7	9.2	41	62	5.7	0	1.3	0.1	277
July	19.5	27.6	11.5	23	57	3.6	0	0.8	0	320
August	19.5	27.5	11.5	23	58	3.4	0	1.3	0	292
September	16.1	23.3	8.9	38	65	5.3	0	1.7	0.1	220
October	11.5	17.2	5.9	60	74	8.3	0	2.9	1.9	151
November	6.6	10.9	2.1	60	82	8.7	1.7	4.6	9.7	99
December	3.9	7.7	0.2	63	85	9.3	3.4	6	15.0	78

T. Temperature in °C; TM. Maximum temperature in °C; Tm Minimum temperature in °C; R. Rain in mm; H Relative humidity in%; DR. Rainy days; DS Snowy days; DF Foggy days; DH Frost days; I Sunny hours.

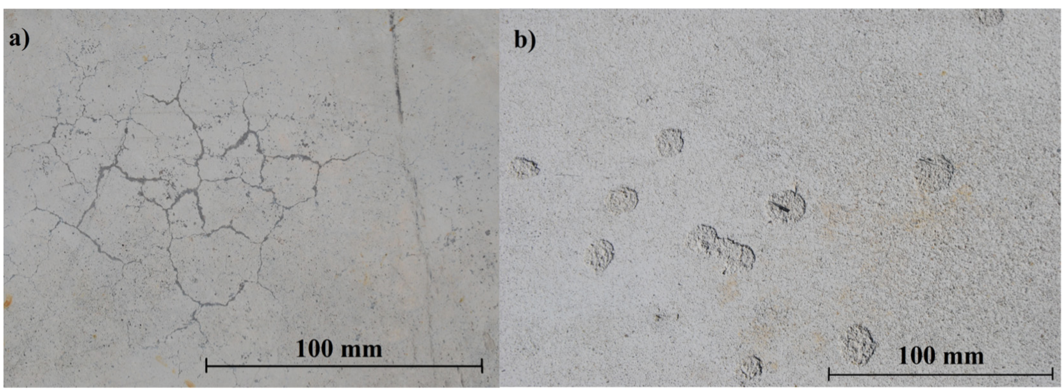

Fig. 7. a) Apparent crazing, mix E. b) Chips found in ES slab.

Table 9
Compressive strength.

	90 days moist room	5 years outdoor	Variation
E	73.7	70.1	−4.9%
EM	79.6	76.3	−4.1%
ES	72.2	69.5	−3.7%

2 mm). It is not decisive for the durability of the slab structure, affecting only its surface appearance. The fact that the cracking appeared in different ways in each slab was due to the different climatic conditions during the casting process. Each slab was built on different days (October 17, October 21 and October 26) and the finishing layer was extended six hours after the pouring of concrete. The main reason for the appearance of this type of crazing is the rate of water evaporation from the surface of the finishing layer during the setting, despite having been covered with a plastic film. The evaporation rate is influenced by the relative humidity of the surrounding air and the wind speed.

Some slight stains were observed in slab EM, due to corrosion of the apparent metallic fibers; in some applications it could be an aesthetic problem and the finishing layer should have been thicker. This phenomenon is a normal event after five years of exposure to weathering, while it is less probable in indoor situations.

The presence of some chips (see Fig. 7b) was observed in slab ES, in a few zones of the slab surface (about 20% of the upper surface). The origin of the chips is not totally clear, but it may be attributed to an interaction between the polymeric fibers and the finished surface, because a fiber presence might be observed in some (but not in all) of them. It is possible that the interaction of the polymeric fibers, the water they absorbed, and the sunshine provoked zones with high water vapor pressure near the upper surface.

6.2. Compressive strength

Three cores of 75 × 150 mm were drilled in each slab to evaluate the compressive strength of the "real" concrete mixes, following the instructions in standard EN 12390-3 [70]. The average compressive strength value of the drilled cores, taken from slabs weathered for 5 years, versus the compressive strength of the 15 0 × 300 mm cylinders of the same mixes, cured in the climatic chamber and tested after 90 days, are shown in Table 9.

The compressive strengths of the slabs after 5 years and of the specimens cured for 90 days in the moist room were fairly similar, considering the inherent loss of strength, due to outdoor weathering of the slabs, and considering the influence of the different specimen sizes. In summary, the three slabs may be said to have resisted the adverse climatic conditions after five years and still show reliable mechanical behavior.

6.3. Impact strength

Three cores per slab were extracted to evaluate the impact strength of each mix after five years of atmospheric exposure. The cores were extracted with a 150 mm-diameter, as specified in the Spanish Standard UNE 83514 [71].

As in the previous article [65], the test results record the number of hits with a steel ball until the first crack and the number of hits until the failure of the specimens. Table 10 presents the results and those previously obtained on laboratory cast specimens tested

Table 10
Impact strength.

	First crack		Failure	
	28 days	5 years	28 days	5 years
E	11	9	13	12
EM	46	18	155	73
ES	24	15	88	62

after 28 days of curing, as prescribed in the aforementioned standard.

It is observed that in all cases the number of hits until the first crack and the breakage decreased in the cores extracted from the slabs. The small decrease in the reference mix can be explained by the different dimensions of the specimens (150 mm cubes at 28 days and cores with a diameter of 150 mm at 5 years) and the damage that the cores might suffer in the extraction process. In the fiber-reinforced concretes, the decrease in the number of hits was more notable. In the opinion of the authors, this decrease is not only related with concrete aging and adverse climatic conditions, but it is also likely to be partially due to fiber orientation and distribution. Fiber distribution is not the same when casting a small size specimen, a slab or a wall, as has been shown by other researchers [55,56]. Finally, the impact strength of the weathered concrete slabs was excellent for the mixes that included fibers with respect to reference mix E.

7. Conclusions

The conclusions of this work can be summarized as follows:

- Steel-slag concrete mixes reinforced with either metallic or synthetic fibers have shown good physical and mechanical properties, with progressive gains throughout the curing time.
- MIP analysis and the water absorption by capillarity test have revealed that the fiber-reinforced CEAFS has in general good properties that can withstand aggressive environments. The unreinforced CEAFS showed slightly poorer properties, foreseeing weaker environmental resistance.
- The incorporation of fibers in the CEAFS can be considered very positive throughout the durability tests, obtaining smaller variations of weight, a good appearance of the specimens, and good strength of these concretes after freeze/thaw and wet/dry cycles and when in contact with aggressive agents such as sulfates, carbon dioxide and sulfur dioxide.
- In general the results obtained in the durability tests were slightly better in the CEAFS concretes reinforced with metallic fibers than in those reinforced with synthetic fibers; the unreinforced concrete showing lower durability.
- The outdoor exposure of the slabs made with unreinforced and fiber-reinforced CEAFS to atmospheric weathering reflected the difficulties of scaling up laboratory experiments to full-scale construction works. The concrete mixes also showed good behavior against the natural outdoor environment.

Acknowledgements

The authors wish to express their gratitude to FEDER, to the Junta de Castilla y León (Regional Government) for funding the UIC-231 with the project BU119P17, to the Spanish Ministry (MINECO) for FEDER Funds through project BIA2014-55576-C2-1-R, and to the Basque Government for funding research group IT781/13, thereby contributing to the financing of this research. This research could not have gone ahead without the materials supplied by Hormor-Zestoa, CHRYSO Admixtures, and Bekaert.

References

[1] J.O. Akinmusuru, Potential beneficial uses of steel slag wastes for civil engineering purposes, Resour. Conserv. Recycl. 5 (1) (1991) 73–80.
[2] P.J. Koros, Dusts, scale, slags, sludges... not wastes, but sources of profits, Metall. Mater. Trans. B: Process Metall. Mater. Process Sci. 34 (6) (2003) 769–779.
[3] W.M. Shelburne, D.J. Degroot, The use of waste & recycled materials in highway construction, Civ. Eng. Pract. 13 (1) (1998) 5–16.
[4] F. Maghool, A. Arulrajah, Y.J. Du, S. Horpibulsuk, A. Chinkulkijniwat, Environmental impacts of utilizing waste steel slag aggregates as recycled road construction materials, Clean Technol. Environ. Policy 19 (4) (2017) 949–958.
[5] C. Pellegrino, P. Cavagnis, F. Faleschini, K. Brunelli, Properties of concretes with black/oxidizing electric arc furnace slag aggregate, Cem. Concr. Compos. 37 (1) (2013) 232–240.
[6] E. Anastasiou, K. Georgiadis Filikas, M. Stefanidou, Utilization of fine recycled aggregates in concrete with fly ash and steel slag, Constr. Build. Mater. 50 (2014) 154–161.
[7] M. Etxeberria, C. Pacheco, J.M. Meneses, I. Berridi, Properties of concrete using metallurgical industrial by-products as aggregates, Constr. Build. Mater. 24 (9) (2010) 1594–1600.
[8] I. Papayianni, E. Anastasiou, Production of high-strength concrete using high volume of industrial by-products, Constr. Build. Mater. 24 (8) (2010) 1412–1417.
[9] M. Pasetto, N. Baldo, Mix design and performance analysis of asphalt concretes with electric arc furnace slag, Constr. Build. Mater. 25 (8) (2011) 3458–3468.
[10] J.T. San José, A. Uría, Escorias de horno de arco eléctrico en mezclas bituminosas, Arte y Cemento 1905 (2001) 122–125.
[11] M. Pasetto, N. Baldo, Fatigue performance of asphalt concretes made with steel slags and modified bituminous binders, Int. J. Pave. Res. Technol. 6 (4) (2013) 294–303.
[12] M. Pasetto, N. Baldo, Resistance to permanent deformation of base courses asphalt concretes made with RAP aggregate and steel slag, in: 12th International Conference on Asphalt Pavements, ISAP 2014, Taylor and Francis – Balkema, Raleigh, NC, 2014, pp. 1199–208.
[13] M. Skaf, J.M. Manso, Á. Aragón, J.A. Fuente-Alonso, V. Ortega-López, EAF slag in asphalt mixes: a brief review of its possible re-use, Resour. Conserv. Recycl. 120 (2017) 176–185.
[14] H. Motz, J. Geiseler, Products of steel slags an opportunity to save natural resources, Waste Manage. 21 (3) (2001) 285–293.
[15] J. Geiseler, Use of steelworks slag in Europe, Waste Manage. 16 (1–3) (1996) 59–63.
[16] G. Wang, Y. Wang, Z. Gao, Use of steel slag as a granular material: volume expansion prediction and usability criteria, J. Hazard. Mater. 184 (1–3) (2010) 555–560.
[17] İ. Yüksel, A review of steel slag usage in construction industry for sustainable development, Environ. Dev. Sustainability 19 (2) (2017) 369–384.
[18] D.H. Le, Y.N. Sheen, Q.B. Bui, An assesment on volume stabilization of mortar with stainless steel slag sand, Constr. Build. Mater. 155 (2015) 200–208.
[19] Steel Statistical Yearbook: World Steel Association, 2014.
[20] EUROSLAG, The European Slag Association. Position Paper on the Status of Ferrous Slag, 2013.
[21] F.A. López, A. López-Delgado, N. Balcázar, Physico-chemical and mineralogical properties of EAF and AOD Slags, Afinidad 53 (461) (1996) 39–46.
[22] L.M. Juckes, The volume stability of modern steelmaking slags, Trans. Inst. Min. Metall. Sect. C. 112 (3) (2003) 177–197.
[23] D.C. Goldring, L.M. Juckes, Petrology and stability of steel slags, Ironmaking Steelmaking 24 (6) (1997) 447–456.
[24] I. Arribas, A. Santamaría, E. Ruiz, V. Ortega-López, J.M. Manso, Electric arc furnace slag and its use in hydraulic concrete, Constr. Build. Mater. 90 (2015) 68–79.
[25] M. Frías Rojas, J.T. San-José, I. Vegas, Árido siderúrgico en hormigones: proceso de envejecimiento y su efecto en compuestos potencialmente expansivos, Mater. Constr. 60 (297) (2010) 33–46.
[26] J. Setién, D. Hernández, J.J. González, Characterization of ladle furnace basic slag for use as a construction material, Constr. Build. Mater. 23 (5) (2009) 1788–1794.
[27] M. Skaf, V. Ortega-Lopez, J.A. Fuente-Alonso, A. Santamaria, J.M. Manso, Ladle furnace slag in asphalt mixes, Constr. Build. Mater. 122 (2016) 488–495.
[28] J.M. Manso, J.A. Polanco, M. Losañez Gonzalez, J.J. Gonzalez, Ladle furnace slag in construction, J. Mater. Civ. Eng. 17 (2005) 513–518.
[29] V. Ortega-López, J.M. Manso, I.I. Cuesta, J.J. González, The long-term accelerated expansion of various ladle-furnace basic slags and their soil-stabilization applications, Constr. Build. Mater. 68 (2014) 455–464.
[30] J.M. Manso, V. Ortega-López, J.A. Polanco, J. Setién, The use of ladle furnace slag in soil stabilization, Constr. Build. Mater. 40 (2013) 126–134.
[31] J.M. Montenegro, M. Celemín-Matachana, J. Cañizal, J. Setién, Ladle furnace slag in the construction of embankments: expansive behavior, J. Mater. Civ. Eng. 25 (8) (2013) 972–979.
[32] F. Maghool, A. Arulrajah, S. Horpibulsuk, Y.J. Du, Laboratory evaluation of ladle furnace slag in unbound pavement-base/subbase applications, J. Mater. Civ. Eng. 29 (2) (2017).
[33] V.Z. Serjun, A. Mladenovič, B. Mirtič, A. Meden, J. Ščančar, R. Milačič, Recycling of ladle slag in cement composites: environmental impacts, Waste Manage. 43 (2015) 376–385.

[34] V.Z. Serjun, B. Mirtič, A. Mladenovič, Evaluation of ladle slag as a potential material for building and civil engineering, Mater. Tehnol. 47 (5) (2013) 543–550.
[35] I. Santamaria-Vicario, A. Rodriguez, S. Gutierrez-Gonzalez, V. Calderon, Design of masonry mortars fabricated concurrently with different steel slag aggregates, Constr. Build. Mater. 95 (2015) 197–206.
[36] J.M. Manso, J.J. Gonzalez, J.A. Polanco, Electric arc furnace slag in concrete, J. Mater. Civ. Eng. 16 (6) (2004) 639–645.
[37] S.I. Abu-Eishah, A.S. El-Dieb, M.S. Bedir, Performance of concrete mixtures made with electric arc furnace (EAF) steel slag aggregate produced in the Arabian Gulf region, Constr. Build. Mater. 34 (2012) 249–256.
[38] J.M. Manso, D. Hernández, M.M. Losáñez, J.J. González, Design and elaboration of concrete mixtures using steelmaking slags, ACI Mater. J. 108 (6) (2011) 673–681.
[39] I. Papayianni, E. Anastasiou, Concrete incorporating highcalcium fly ash and EAF slag aggregates, Mag. Concr. Res. 63 (8) (2011) 597–604.
[40] J.T. San-José, I. Vegas, I. Arribas, I. Marcos, The performance of steel-making slag concretes in the hardened state, Mater. Des. 60 (2014) 612–619.
[41] H. Sasamoto, A. Tsubone, Y. Kamiya, K. Sano, Development of fishing block using EAF refining slag, Tetsu-To-Hagane/J. Iron Steel Inst. Jpn. 89 (4) (2003) 461–465.
[42] S. Monosi, M.L. Ruello, D. Sani, Electric arc furnace slag as natural aggregate replacement in concrete production, Cem. Concr. Compos. 66 (2016) 66–72.
[43] C. Pellegrino, F. Faleschini, Experimental behavior of reinforced concrete beams with electric arc furnace slag as recycled aggregate, ACI Mater. J. 110 (2) (2013) 197–205.
[44] S.W. Kim, Y.J. Lee, K.H. Kim, Bond behavior of RC beams with electric arc furnace oxidizing slag aggregates, J. Asian Arch. Build. Eng. 11 (2) (2012) 359–366.
[45] J.M. Manso, J. Setién, Investigación de nuevos usos de las escorias de horno eléctrico de arco (EAF): la oportunidad de los hormigones, Hormigón y acero. 241 (2006) 51–57.
[46] C. Pellegrino, F. Faleschini, Experimental investigation on RC beams containing slag as recycled aggregate, in: fib Symposium 2012: Concrete Structures for Sustainable Community, Stockholm, 2012, pp. 451–454.
[47] S.-W. Kim, Y.-J. Lee, Y.-H. Lee, K.-H. Kim, Flexural performance of reinforced high-strength concrete beams with EAF oxidizing slag aggregates, J. Asian Arch. Build. Eng. 15 (3) (2016) 589–596.
[48] F. Faleschini, M. Alejandro Fernández-Ruíz, M.A. Zanini, K. Brunelli, C. Pellegrino, E. Hernández-Montes, High performance concrete with electric arc furnace slag as aggregate: mechanical and durability properties, Constr. Build. Mater. 101 (2015) 113–121.
[49] F. Faleschini, L. Hofer, M.A. Zanini, M. dalla Benetta, C. Pellegrino, Experimental behavior of beam-column joints made with EAF concrete under cyclic loading, Eng. Struct. 139 (2017) 81–95.
[50] M.N.T. Lam, S. Jaritngam, D.H. Le, Roller-compacted concrete pavement made of electric arc furnace slag aggregate: mix design and mechanical properties, Constr. Build. Mater. 154 (2017) 482–495.
[51] E.K. Anastasiou, I. Papayianni, M. Papachristoforou, Behavior of self compacting concrete containing ladle furnace slag and steel fiber reinforcement, Mater. Des. 59 (2014) 454–460.
[52] A. Santamaría, A. Orbe, M. Losañez, M. Skaf, V. Ortega López, J. Gonzalez, Self-compactin concrete incorporating electric arc-furnace steelmaking slag as aggregate, Mater. Des. 115 (2017) 179–193.
[53] S.P. Shah, J.I. Daniel, S. Ahmad, M. Arockiasamy, P. Balaguru, C. Ball, et al., Guide for specifying, proportioning, mixing, placing, and finishing steel fiber reinforced concrete, ACI Mater. J. 90 (1) (1993) 94–101.
[54] A. Orbe, J. Cuadrado, R. Losada, E. Rojí, Framework for the design and analysis of steel fiber reinforced self-compacting concrete structures, Constr. Build. Mater. 35 (2012) 676–686.
[55] A. Orbe, R. Losada, E. Rojí, J. Cuadrado, A. Maturana, The prediction of bending strengths in SFRSCC using computational fluid dynamics (CFD), Constr. Build. Mater. 66 (2014) 587–596.
[56] A. Blanco, P. Pujadas, A. De La Fuente, S.H.P. Cavalaro, A. Aguado, Assessment of the fibre orientation factor in SFRC slabs, Composites Part B 68 (2015) 343–354.
[57] K.H. Khayat, Y. Roussel, Testing and performance of fiber-reinforced, selfconsolidating concrete, Mater. Struct./Mater. Constr. 33 (230) (2000) 391–397.
[58] V. Bharath, P. Rao, Study on the fibre reinforced concrete using steel slag as the coarse aggregate replacement, Int. J. Technol. Res. Eng. 2 (7) (2015).
[59] A. Llano-Torre, S.E. Arango, E. García-Taengua, J.R. Martí-Vargas, P. Serna, Influence of fibre reinforcement on the long-term behaviour of cracked concrete, RILEM Bookseries: Kluwer Academic Publishers, 2017, pp. 195–209.
[60] S. Grünewald, F. Laranjeira de Oliveira, J. Walraven, A. Aguado de Cea, C. Molins i Borrell, Influence of fibre orientation on the performance of steel fibre-reinforced concrete, in: Eighth RILEM International Symposium on Fibre Reinforced Concrete (BEFIB 2012), Guimarães, Portugal: International Union of Laboratories and Experts in Construction Materials, Systems and Structures (RILEM), 2012, pp. 1–12.
[61] A.S. El-Dieb, Mechanical, durability and microstructural characteristics of ultra-high-strength self-compacting concrete incorporating steel fibers, Mater. Des. 30 (10) (2009) 4286–4292.
[62] A.S. El-Dieb, M.M. Reda Taha, Flow characteristics and acceptance criteria of fiber-reinforced self-compacted concrete (FR-SCC), Constr. Build. Mater. 27 (1) (2012) 585–596.
[63] P. Bosela, N. Delatte, R. Obratil, A. Patel, Fresh and hardened properties of paving concrete with steel slag aggregate, Propiedades para firmes del hormigón fabricado con áridos siderúrgicos, Carreteras 4 (166) (2009) 55–66.
[64] I. Arribas, J. San-José, I. Vegas, J. Hurtado, J. Chica, Application of steel slag concrete in the foundation slab and basement wall of the Tecnalia kubik building, in: 6th European Slag Conference Proceedings. Madrid, Euroslag, 2010, pp. 251–264.
[65] J.A. Fuente-Alonso, V. Ortega-López, M. Skaf, A. Aragón, J.T. San-José, Performance of fiber-reinforced eaf slag concrete for use in pavements, Constr. Build. Mater. 149 (2017) 629–638.
[66] J.M. Manso, J.A. Polanco, M. Losañez, J.J. González, Durability of concrete made with EAF slag as aggregate, Cem. Concr. Compos. 28 (6) (2006) 528–534.
[67] J.A. Polanco, J.M. Manso, J. Setién, J.J. González, Strength and durability of concrete made with electric steelmaking slag, ACI Mater. J. 108 (2) (2011) 196–203.
[68] I. Arribas, I. Vegas, J.T. San-José, J.M. Manso, Durability studies on steelmaking slag concretes, Mater. Des. 63 (2014) 168–176.
[69] C. Pellegrino, V. Gaddo, Mechanical and durability characteristics of concrete containing EAF slag as aggregate, Cem. Concr. Compos. 31 (9) (2009) 663–671.
[70] EN Euronorm, Rue de Stassart, 36. Belgium–1050 Brussels: European Committee for Standardization.
[71] UNE Spanish Standars, AENOR, Madrid, Spain.
[72] Annual Book of ASTM Standars, ASTM International, West Conshohocken, 19429-2959, PA, USA, 2008.
[73] M. Blanco-Varela, J. Aguilera, S. Martínez Ramírez, A. Palomo, C. Riontino, G. Zappia, Thaumasite formation in hydraulic mortars by atmospheric SO_2 deposition, Mater. Constr. 51 (263–4) (2001) 109–125.